Quaternary Research 76 (2011) 430–440

Contents lists available at ScienceDirect

Quaternary Research

journal homepage: www.elsevier.com/locate/yqres

Chronostratigraphy and lake-level changes of Laguna Cari-Laufquén, Río Negro, Argentina

Alyson Cartwright [a,*], Jay Quade [a], Scott Stine [b], Kenneth D. Adams [c], Wallace Broecker [d], Hai Cheng [e,f]

[a] University of Arizona, Department of Geosciences, Tucson, AZ, 85721, USA
[b] California State University East Bay, Department of Geography and Environmental Sciences, Hayward, CA, 94542, USA
[c] Desert Research Institute, Division of Earth and Ecosystem Sciences, Reno, NV, 89512, USA
[d] Columbia University, Lamont-Doherty Earth Observatory, New York, NY, 10027, USA
[e] University of Minnesota, Department of Geology and Geophysics, Minneapolis, MN, 55455, USA
[f] Institute of Global Environmental Change, Xi'an Jiaotong University, Xi'an, Shaanxi 710049, China

ARTICLE INFO

Article history:
Received 29 December 2010
Available online 27 August 2011

Keywords:
Argentina
Paleolakes
Carbon-14
Last glacial maximum
Shoreline

ABSTRACT

Evidence from shoreline and deep-lake sediments show Laguna Cari-Laufquén, located at 41°S in central Argentina, rose and fell repeatedly during the late Quaternary. Our results show that a deep (>38 m above modern lake level) lake persisted from no later than 28 ka to 19 ka, with the deepest lake phase from 27 to 22 ka. No evidence of highstands is found after 19 ka until the lake rose briefly in the last millennia to 12 m above the modern lake, before regressing to present levels. Laguna Cari-Laufquén broadly matches other regional records in showing last glacial maximum (LGM) highstands, but contrasts with sub-tropical lake records in South America where the hydrologic maximum occurred during deglaciation (17–10 ka). Our lake record from Cari-Laufquén mimics that of high-latitude records from the Northern Hemisphere. This points to a common cause for lake expansions, likely involving some combination of temperature depression and intensification of storminess in the westerlies belt of both hemispheres during the LGM.

Introduction

Street and Grove (1979) were among the first to compile worldwide lake records to gain perspective on changes in global paleoclimate. Their compilations showed strong differences in the timing of lake-level changes at low and high latitudes, that is, between lakes in the westerly (mid-latitude) and easterly (low-latitude) windbelts. It is now widely recognized that many mid- to high latitude lakes and glaciers in the Northern Hemisphere experienced significant expansions during the last glacial maximum (24–18 ka) and late glacial period (17–12 ka). This is also thought to be the case for glaciers in the Southern Hemisphere, leading many to suggest the causes are not simple orbital forcing, since such forcings are hemispherically out-of-phase (Mercer, 1984; Lowell et al., 1995; Denton et al., 1999).

Hydrologic modeling of desert lakes in the Northern Hemisphere points to some combination of much (−6°C) cooler temperatures and modest increases in precipitation as a cause for lake expansions during the LGM (Benson et al., 1990; Bartov et al., 2002; Jones et al., 2007). The causes of rainfall increase are not clear. It has long been argued that in western North America, a significant (15°) southward shift of the mean position of the westerlies, in response to ice-sheet growth and splitting of the jet stream, was the source of enhanced rainfall (Antevs, 1948; Hostetler and Benson, 1990). High-latitude lakes in southern South America also appear to have expanded at this time (e.g., Markgraf et al., 2007), suggesting a common cause with lake expansions in the Northern Hemisphere.

A different explanation for increased glacial-age rainfall in the high latitudes is embedded in the recent observations of physical climatologists who suggest that rainfall and temperature in deserts are inversely linked (Held and Soden, 2006). Here it has been suggested that rainfall in the mid-latitude deserts will decrease as the Earth warms, and conversely, on a colder planet, the same deserts will be wetter. In a recent survey of global paleolakes, Quade and Broecker (2009) found significant support for this linkage, while recognizing that many lake-level histories are not well dated enough, or properly located, for a robust test of either hypothesis (westerlies shift versus temperature-related rainfall increase).

One important but relatively unstudied region for examining these ideas is southern South America. We selected Laguna Cari-Laufquén for study because of its advantageous location in the region (Fig. 1), allowing for the test of a shifting windbelt, depressed temperatures, or other climate factors as reasons for lake growth during the Quaternary. At present, Laguna Cari-Laufquén is near the current average position of the southern westerlies (~40°S) in southern Argentina (Markgraf, 1993, 1998).

Our study focuses on shoreline deposits rather than the more traditional core-based evidence. Even though shoreline deposits will

* Corresponding author.
E-mail address: alysonc@email.arizona.edu (A. Cartwright).

0033-5894/$ – see front matter © 2011 University of Washington. Published by Elsevier Inc. All rights reserved.
doi:10.1016/j.yqres.2011.07.002

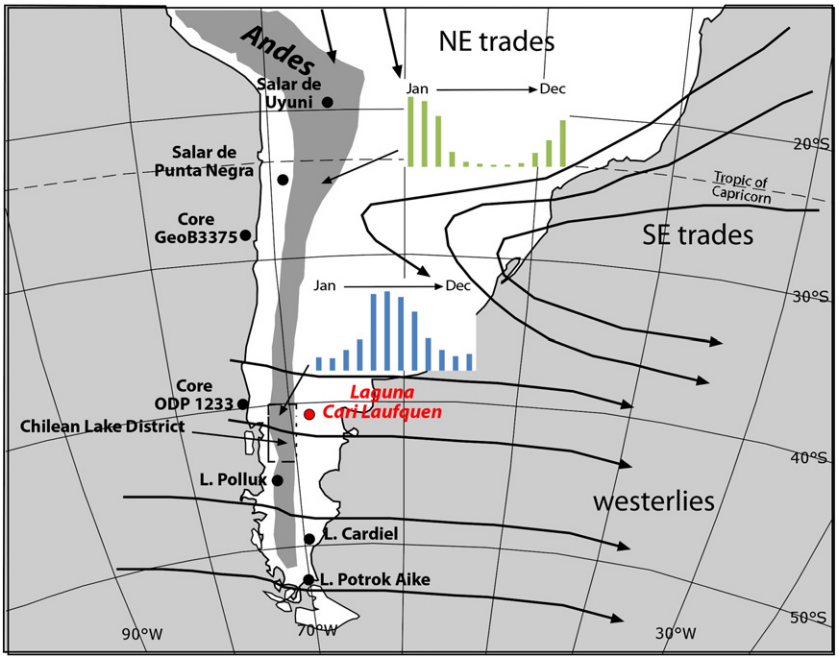

Fig. 1. Map of South America showing the general current position of the westerlies and easterlies, location of the Cari-Laufquén study site, and other sites discussed in this paper. Histograms show relative modern monthly precipitation from CRU 2.0 CL dataset.

not provide the continuous high-resolution time series of a core, they are ideally suited for capturing large hydrologic change, for unequivocal depth reconstruction, and for precise age control. All of these characteristics lend well to determining wet or dry trends on the long time scales of interest to us here. After Lago Cardiel (Stine and Stine, 1990), ours is the only other published paleoshoreline study in central and southern Patagonia.

Laguna Cari-Laufquén was studied previously at a reconnaissance level by Galloway et al. (1988) and Whatley and Cusminsky (1999). These papers report six radiocarbon dates and one thermoluminescence date used to infer development of a fresh-water paleolake ranging from 15 to 30 m above current lake level between 18 and 22 ka, and a much shallower (+8 m) lake in the early Holocene. The extensive lacustrine exposures in the basin invite a much more systematic study of the lake history.

Regional climate

Modern rainfall in southern Patagonia is dominated by winter storms that appear to derive mainly from the Atlantic Ocean (Fig. 1). Winter rainfall today is anti-phased with westerly wind strength: strong westerly winds enhance rainfall west of the Andes but tend to suppress it on the eastern rainshadow (Patagonian) side of the Andes (Garreaud, 2007; Moy et al., 2009). At present, the westerly storm track centers around 40°S during July (austral winter) and migrates poleward during December (austral summer) to around 45°S (Markgraf, 1993, 1998). Seasonal average temperatures range from 2°C in the austral winter to 16.5°C in the austral summer, with an annual average just over 9°C. Modern precipitation is 284 mm/yr, with over 50% of the yearly total arriving May through August (CRU CL 2.0 data set). This pattern of winter-dominated rainfall is shown in Fig. 1, highlighting the dominance of summer rainfall farther to the north of Cari-Laufquén and winter precipitation in the south.

Physical setting and lacustrine deposits

The Laguna Cari-Laufquén basin is located in Rio Negro Province in central Argentina at about 41°S and 70°W. The hydrographic basin covers 13,546 km^2 (Graham et al., 1999) and is drained by the perennial Rio Maquinchao, which is nourished by snowmelt and rainfall mainly from the low mountains on the west and south sides of the basin. Two lakes, Cari-Laufquén Grande and Cari-Laufquén Chica, occupy the basin bottom, referred to hereafter as Laguna Grande and Laguna Chica (Fig. 2). The basin is and was hydrographically closed; at no point did paleolakes spill out externally. The Rio Maquinchao first empties into Laguna Chica, which is 5.89 km^2 in area, stands at about 825 m elevation, and is about 8 m deep (Reissig et al., 2006). Laguna Chica overflows to the north, feeding the lower Rio Maquinchao, which then flows into Laguna Grande. Laguna Grande fluctuates in size and depth, but at the time of our study in 2007 it covered 30.75 km^2, stood at an elevation of 786 m asl, and is reported to be about 8–10 m deep (Reissig et al., 2006). The basin is underlain largely by Tertiary volcanic rocks, although older siliclastic sedimentary rocks are locally exposed beneath the volcanic rocks. There are no apparent carbonate rocks exposed in the basin.

Evidence for ancient lakes in the basin is visible along the lower Rio Maquinchao, with exposures of up to 7 m of lacustrine sediment in many places and as conspicuous gravelly beach ridges, especially along the east side of the basin (Fig. 2). The Rio Maquinchao exposures extend up to about 826 m (+40 m above the current lake, or acl); above that, gravel barriers, silt-covered back-barrier depressions, and scattered lacustrine tufa are the main physical expression of the paleolakes. There are a number of paleoshorelines visible on aerial imagery, but the main ones are the very prominent “lowway” and “highway” shoreline couplet at 839 m (+53 m acl) and 841 m (+55 m acl), and the “high” berm at 847.5 m (+61.5 m acl), all of these extending for more than 20 km on the east side of the basin (Figs. 2, 3).

The other prominent paleolake feature is tufa, which takes the form of floral-like heads (Fig. 4a), and coatings on cobbles several millimeters up to a centimeter thick. The tufa is most abundant at 822–824 m (+36–38 m acl) elevation, in many places such as Cerro Ambrosio, and at CL-22 and CL-5 (Fig. 2). Another common occurrence is reworked chips of tufa in the gravels of the lowway and highway shorelines. Finally, coatings of tufa are common on

https://doi.org/10.1016/j.yqres.2011.07.002 Published online by Cambridge University Press

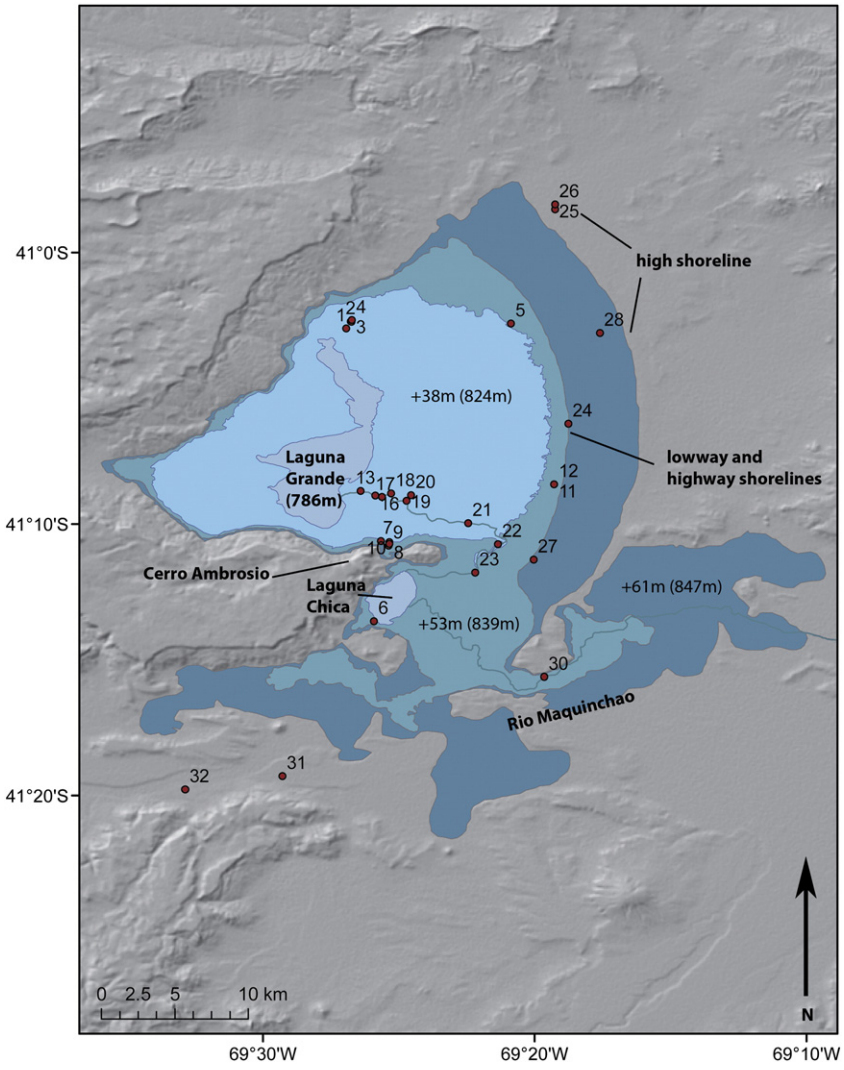

Fig. 2. The Laguna Cari-Laufquén area showing the main landmarks and numbered sample sites, prefixed with CL- throughout the tables and text of this paper. Prominent shorelines discussed in text are indicated. Various shades indicate reconstructed lake levels with corresponding elevations. See Fig. 1 for regional location of Laguna Cari-Laufquén.

cobbles found around the modern lake (Fig. 2, CL-1, -3, -24) on very young shorelines within 3 m of the current level of Laguna Grande.

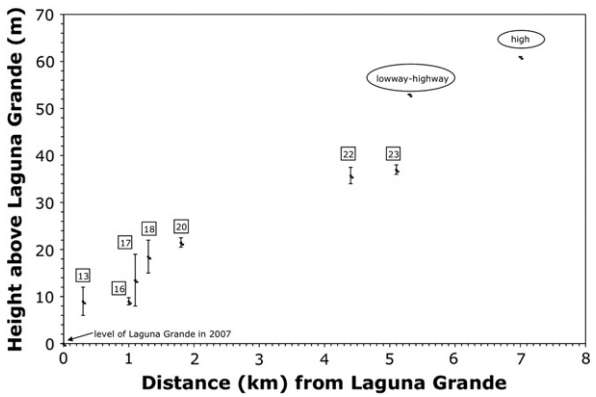

Fig. 3. Cross-section of the stratigraphic sections (numbered in boxes; see Fig. 7) and main paleoshorelines (circled) in the study area relative to the level of Laguna Grande (786 m asl in 2007). This section runs approximately east–west along the lower Rio Maquinchao between Laguna Grande to the west to the paleoshoreline complexes exposed along the east side of the basin (Fig. 2).

Methods

Elevations

We measured elevations using a barometric altimeter and hand-held Wide Area Augmentation Service (WAAS)-enabled GPS receiver with a resettable barometric altimeter. We located several surveyed benchmarks in our area of known elevation, and calibrated our altimeter and GPS receiver to these elevations each morning. This calibration could drift in the course of the day as the afternoon winds picked up, so we either recalibrated or confined our elevation measurements to the early morning hours. Reproducibility between altimeters in such conditions was on the order of ± 1 m in a given morning, but could be up to ± 2 m with repeat measurements from day to day. We take ± 2 m as the error on our elevation measurements presented in this paper (Supplementary Table 1). We will express elevations both with respect to sea level followed in parentheses by the number of meters above the 2007 height of Laguna Grande, estimated to be 786 m asl.

Stable isotope analyses

Lacustrine carbonates were ground then heated at 250°C for 3 h in vacuo before stable isotopic analysis using an automated sample

https://doi.org/10.1016/j.yqres.2011.07.002 Published online by Cambridge University Press

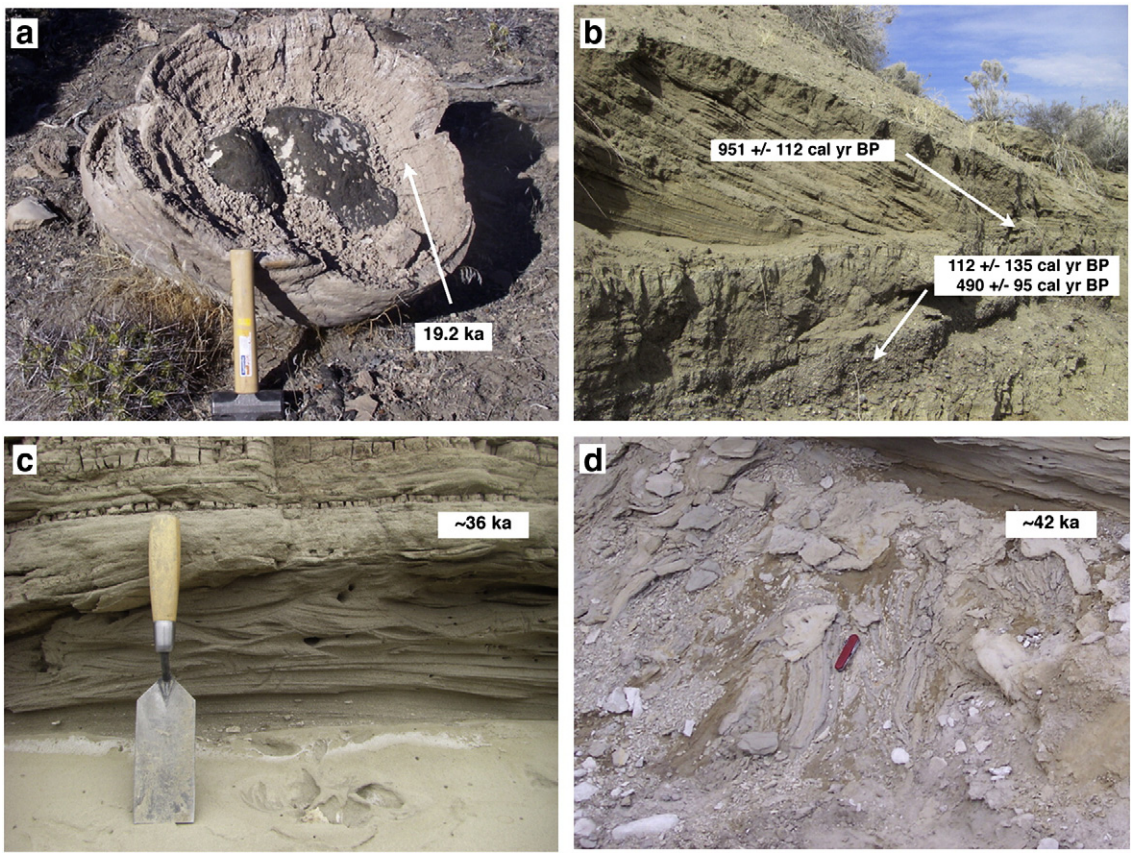

Fig. 4. a) A large tufa head from about 824 m at Cerro Ambrosio (Fig. 2). It dates to 19.2 cal yr BP (Table 1: CL-7C). Tufas at about this elevation throughout the basin date in the 19.2–20.7 ka range; b) Photo from CL-13 (Fig. 2) showing the lowest and youngest lake cycle represented by Unit E. The large-scale cross-beds of Unit E overlie channel gravels and bedded silt of Unit D, which dates to 100–400 cal yr BP; c) Base of Unit A exposed near CL-18, showing ripple cross-bedded sands near the base formed within wave base, capped by laminated silt deposited in deep water; and d) soft-sediment deformation in sands in the middle of Unit A, CL-17 (Fig. 7).

preparation device (Kiel III) attached directly to a Finnigan MAT 252 mass spectrometer at the University of Arizona. Measured $\delta^{18}O$ and $\delta^{13}C$ values were corrected using internal laboratory standards calibrated to NBS-19 based on internal lab standards. Precision of repeated standards is $\pm 0.11‰$ for $\delta^{18}O$ (1σ). Carbonate isotopic results are reported using standard δ-per mil notation relative to VPDB.

Unfiltered lake, spring, and river water were sealed with Teflon and electrician's tape into a 15-ml centrifuge tube and refrigerated in the laboratory. $\delta^{18}O$ (SMOW) of water samples were measured using the CO_2 equilibration method on an automated sample preparation device attached directly to a Finnigan Delta S mass spectrometer at the University of Arizona. The δD values of water were measured using an automated chromium reduction device (H-Device) attached to the same mass spectrometer. The values were corrected based on internal lab standards, which are calibrated to SMOW and SLAP. The analytical precision for $\delta^{18}O$ and δD measurements is 0.08‰ and 0.6‰, respectively (1σ). Water isotopic results are reported using standard δ-per mil notation relative to SMOW.

Carbon-14 dating

Shell, tufa, and calcareous sediment was cleaned ultrasonically, soaked in ~2% H_2O_2, and rinsed thoroughly in distilled water. The intact material was converted to CO_2 using 100% H_3PO_4 under vacuum. Dissolved inorganic carbon (DIC) was extracted by hydrolysis of ~500 ml of water collected in sealed containers. Dating was carried out by the University of Arizona Accelerator Mass Spectrometer Facility. For conversion of carbon-14 dates (expressed as ^{14}C yr BP) to calendar ages (expressed as cal yr BP), CALIB 6.0 (IntCal09) (Stuiver and Reimer, 1993; Reimer et al., 2009) was used to generate a median and a 2-sigma probability range for each ^{14}C date in calendar years (Table 1).

Uranium–thorium dating

The ^{230}Th dating work was performed on a multi-collector inductively coupled plasma mass spectrometer (MC-ICPMS, Thermo-Finnigan Neptune) in the Minnesota isotope laboratory, University of Minnesota. The chemical procedures used to separate the uranium and thorium for ^{230}Th dating are similar to those described in Edwards et al. (1987). Uranium and thorium isotopes were analyzed on the multiplier behind the retarding potential quadrupole (RPQ) in peak-jumping mode. Instrumental mass fractionation was determined by measurements of a ^{233}U–^{236}U spike. The detail techniques are similar to those described in Cheng et al. (2000, 2009) and half-life values are those reported in Cheng et al. (2008).

Results

Dating results and considerations

We dated the deposits at Cari-Laufquén using two radiometric systems—carbon-14 (Table 1) and U/Th (Table 2)—as an independent check of our results.

Carbon-14

Various forms of carbonate—mollusks, ostracodes, tufa, and calcareous sediment—are the only widely available material for dating of sedimentary deposits at Cari-Laufquén. For the carbonates

https://doi.org/10.1016/j.yqres.2011.07.002 Published online by Cambridge University Press

Table 1
^{14}C results from Cari-Laufquén.

Sample #	AMS #	Type	Elev. above lake (m)[a]	$\delta^{13}C$	Fmc[b]	^{14}C age (yr BP)	Cal yr BP[c]	+	−
Chica DIC	AA84777	DIC	0	2.5	1.0549 ± 0.0021	Post-bomb	Modern		
Grande DIC	AA84776	DIC	0	−0.4	1.0682 ± 0.0021	Post-bomb	Modern		
CL-02	AA82119	Tufa	0.5	2.1	1.1644 ± 0.0037	Post-bomb	Modern		
CL-03	AA82116	Tufa	1.7	1.6	0.9989 ± 0.0031	10 ± 30	54	206	28
CL-04	AA82117	Tufa	1.7	0.7	0.9985 ± 0.003	10 ± 20	51	203	19
CL-05	AA79944	Tufa	31	3.5	0.1121 ± 0.0008	17,580 ± 60	20,743	521	333
CL-07a	AA80653	Tufa	38	3.0	0.1218 ± 0.0013	16,910 ± 80	20,044	311	219
CL-07b	AA79945	Tufa	38	3.7	0.1367 ± 0.0009	15,980 ± 60	19,150	264	202
CL-07C-01	AA80651	Tufa	38	3.0	0.1357 ± 0.0013	16,040 ± 80	19,216	248	253
CL-07C-05	AA80652	Tufa	38	3.0	0.1354 ± 0.0012	16,060 ± 70	19,238	224	253
CL-08	AA79946	Tufa	38	3.7	0.1212 ± 0.0010	16,950 ± 70	20,079	288	223
CL-09	AA80654	Tufa	45	3.0	0.1242 ± 0.0010	16,750 ± 60	19,910	297	342
CL-10	AA80655	Tufa	43.9	3.0	0.1199 ± 0.0014	17,040 ± 90	20,166	357	295
CL-13a	AA80658	Planoribid	6	−25.0	0.9782 ± 0.0011	180 ± 10	182	103	187
CL-13c	AA80659	Succineid	6	−25.0	0.9838 ± 0.0022	130 ± 20	117	165	111
CL-13d(a)	AA80660	Succineid	6	−25.0	0.9872 ± 0.0034	100 ± 30	112	166	104
CL-13d(b)	AA82114	Planorbid	6	3.3	0.9508 ± 0.0029	410 ± 20	490	30	160
CL-13e	AA82113	Succinieid	6	3.3	0.8783 ± 0.0028	1040 ± 30	951	109	149
CL-14	AA80657	Mollusk-undent.	0	3.0	0.62490.0017	3780 ± 20	4151	96	151
CL-15	AA80656	Mollusk-undent.	0	3.0	0.6550 ± 0.0036	3400 ± 40	3649	181	169
CL-16a(a)	AA82112	Succineid	8	−5.9	0.954 ± 0.0003	380 ± 0	476	24	139
CL-16a(b)	AA83597	Lymnaed	8	−7.9	0.9689 ± 0.0029	250 ± 20	295	134	300
CL-17d	AA82122	Bulk sand	12	−5.7	0.0098 ± 0.0004	37,170 ± 290	41,980	485	485
CL-17e	AA84773	Ostracod	14	1.0	0.0600 ± 0.0012	22,600 ± 160	27,316	574	574
CL-18b	AA82121	Ostracod	19	1.4	0.0187 ± 0.0004	31,970 ± 190	36,560	321	321
CL-18k	AA82115	Carbonate sediments	21	3.0	0.0166 ± 0.0004	32,920 ± 210	37,640	822	822
CL-20a	AA83598	Bulk silt	30	0.9	0.0474 ± 0.0013	24,490 ± 20	29,365	189	189
CL-22b	AA83596	Bulk silt	34	2.0	0.0579 ± 0.0014	22,880 ± 190	27,510	636	636
CL-22c	AA82120	Bulk sand	35	2.6	0.0709 ± 0.0008	21,260 ± 90	25,689	311	350
CL-22d	AA79761	Tufa	36	3.7	0.0978 ± 0.0007	18,670 ± 60	22,249	204	204
CL-22e	AA79760	Tufa	36.5	3.9	0.1022 ± 0.0014	18,320 ± 110	21,813	465	758
CL-22f	AA79941	Tufa	37.5	3.0	0.1265 ± 0.0010	16,610 ± 70	19,708	332	218
CL-23a	AA83589	Bulk sand	36.5	2.0	0.0952 ± 0.0011	18,880 ± 90	22,404	314	269
CL-23d	AA82123	Carbonate sediments	37.5	0.8	0.1972 ± 0.0013	13,040 ± 50	15,403	515	388
CL-29a	AA79947	Tufa	58	3.1	0.00888 ± 0.0004	37,940 ± 320	42,481	522	522
CL-29b	AA79948	Tufa	58	3.0	0.01120 ± 0004	36,060 ± 250	41,211	539	539

[a] Elev. above lake (m) = meters above present day Laguna Grande (786 m absolute).
[b] Fmc is fraction modern carbon and includes lab blank correction (specific to each run, or running average).
[c] Calendar years calibrated with CALIB 6.0 — Intcal 09, years B.P. (before present–1950 AD) at 2σ.

we obtained thirty-four radiocarbon dates that range in ^{14}C age from post-bomb to 38,000 ^{14}C yr BP (Table 1). Dissolved inorganic carbon (DIC) in both Lagunas Chica and Grande both yielded post-bomb ages, 1.09 times the ratio in pre-nuclear atmosphere in Laguna Grande. This result lies on the trend for atmospheric CO_2, which is declining as bomb test ^{14}C mixes with carbon in the ocean and terrestrial biosphere.

This and other evidence suggests the ^{14}C reservoir effect in the modern Grande lake is minimal. We dated a series of tufas cemented on rocks associated with very young shorelines within a few meters of the modern lake at 786 m. Tufa coating pebbles on a recently abandoned strandline ~1 m above the current lake also returned a post-bomb result (CL-02). Tufa on other young beach berms at +1.7 and +2 m returned ^{14}C dates of 10 ± 30 and 10 ± 20 ^{14}C yr BP, respectively (CL-03, -04). Dead snail shells near the mouth of the Rio Maquinchao within 1 m of the current lake level returned ages of 3400–3800 ^{14}C yr BP (CL-14, -15). In light of the other evidence from the DIC and tufas, we interpret this shell as reworked from older deposits exposed along the banks of the lower Maquinchao.

Were the paleolakes in ^{14}C equilibrium with the atmosphere, like the modern lake? Modern evaporation rates from the lake are on the order of 720 mm/yr. At that rate, the modern lake at 8 m depth would entirely turn over in a few decades. A 40-m-deep paleolake would require 100–200 years, little time for old ^{14}C buildup in the lake. The modern and ancient lakes also have a very large surface area/volume ratio, and Patagonia is one of the windiest land areas in the world

Table 2
U/Th dating results from Cari-Laufquén.

Sample number	^{238}U (ppb)	^{232}Th (ppt)	^{230}Th/^{232}Th (atomic × 10^{-6})	$\delta^{234}U$[a] (measured)	^{230}Th/^{238}U (activity)	^{230}Th age (yr) (uncorrected)	$\delta^{234}U_{initial}$[b] (corrected)	^{230}Th age (yr) (corrected)
CL-08	1841 ± 4	444,000 ± 9000	17.5 ± 0.4	471.2 ± 2.1	0.2555 ± 0.0018	20,600 ± 200	493 ± 5	15,700 ± 3400
CL-07b	1111 ± 3	521,000 ± 11,000	12.0 ± 0.3	518.2 ± 2.3	0.3421 ± 0.0028	27,400 ± 300	550 ± 10	18,200 ± 6500
CL-05	1344 ± 5	785,000 ± 16,000	10.5 ± 0.2	467.2 ± 2.6	0.3723 ± 0.0036	31,400 ± 400	490 ± 10	19,400 ± 8500
CL-22f(1)	2180 ± 7	761,000 ± 8000	11.2 ± 0.2	440.4 ± 3.1	0.2368 ± 0.0023	19,400 ± 200	456 ± 7	12,200 ± 5100
CL-22f(2)	2530 ± 10	639,000 ± 7000	13.4 ± 0.2	444.0 ± 4.8	0.2047 ± 0.0018	16,500 ± 200	459 ± 7	11,300 ± 3600
CL-22f(3)	2440 ± 10	648,000 ± 7000	13.6 ± 0.2	448.1 ± 4.3	0.2187 ± 0.0020	17,700 ± 200	464 ± 7	12,300 ± 3800
CL-22f(4)	2170 ± 10	1,250,000 ± 12,000	7.6 ± 0.1	413.9 ± 5.8	0.2670 ± 0.0024	22,600 ± 300	430 ± 10	10,200 ± 8900

Corrected ^{230}Th ages assume the initial ^{230}Th/^{232}Th atomic ratio of $4.4 \pm 2.2 \times 10^{-6}$. Those are the values for a material at secular equilibrium, with the bulk earth ^{232}Th/^{238}U value of 3.8. The errors are arbitrarily assumed to be 50%.
[a] $\delta^{234}U = ([^{234}U/^{238}U]_{activity} - 1) \times 1000$.
[b] $\delta^{234}U_{initial}$ was calculated based on ^{230}Th age (T), i.e., $\delta^{234}U_{initial} = \delta^{234}U_{measured} \times e^{\lambda 234 \times T}$.

https://doi.org/10.1016/j.yqres.2011.07.002 Published online by Cambridge University Press

(maximum monthly windspeeds exceed 30 m/s, Miller, 1976). This would have promoted very active overturning and exchange with the atmosphere. Radiocarbon enters the lake via CO_2 exchange with the overlying atmosphere. The average rate of exchange between the ocean and atmosphere is about 22 mol/m^2 yr. Meteorological wind speed data over Cari-Laufquén shows an average 4.1 m/s at two meters above the surface. This would correlate to a CO_2 exchange rate of 11 mol/m^2 yr. Based on a mean paleolake depth of 60 m, the amount of ΣCO_2 per square meter of Cari-Laufquén surface should be <100 mol. Hence the replacement time with respect to exchange with the atmosphere is approximately five years. This being the case, the ^{14}C to C ratio in the deepest paleolake should have been very close to that in the atmosphere.

This conclusion is supported by the absence of carbonate rocks in the drainage basin, and by the high $\delta^{13}C$ (PDB) values of tufas of both the historic (+0 to +1‰) and the late-glacial lake (+2 to +4‰) (Fig. 5). These values are very close to that expected for equilibrium between lake carbonate and recent (−8‰) and pre-recent (−6.5‰) atmospheric CO_2, assuming temperatures of formation of ~10±5°C.

Uranium/thorium

Raw U–Th dates from four tufa samples from the 822–824 m range between 20.5 and 31.4 ka (Table 2). The tufas, although very well preserved, display a distinctive tan color indicative of significant detrital silt and clay content. The presence of contaminating U and Th in our results from these detrital sources is apparent in the very high (>10^{-5}) $^{230}Th/^{232}Th$ ratios of the analytes (Table 2). Various schemes have been proposed for dealing with "correcting" for inherited U and Th. In Table 2 we use a rather generic approach of assuming crustal $^{230}Th/^{232}Th$ ratios, which reduce raw ages by 5–12 ka and yield ages in the 15.7 to 19.4 ka range. Within error these ages largely overlap ^{14}C ages on the same tufas (Table 1). But we stress the large uncertainties associated with these ages (±3 to 9 ka) largely because of the high detrital U and Th content and their uncertain isotopic composition. As such, we do not bring these results into our age reconstructions of the lake history.

Stratigraphy and geochronology of sedimentary units

We distinguish five main stratigraphic units (oldest to youngest: A to E) in the exposures along the Rio Maquinchao. Units were separated largely on the basis of disconformable boundaries, following the example of previous paleolake studies (Morrison, 1978; Morrison, 1991; Placzek et al., 2006). In this sense our stratigraphic units represent distinct alluvial or lacustrine depositional episodes which can be somewhat time-transgressive and quite varied sedimentologically. We present our ^{14}C-based calendar ages for each unit uncorrected for any ^{14}C reservoir effects, as previously discussed.

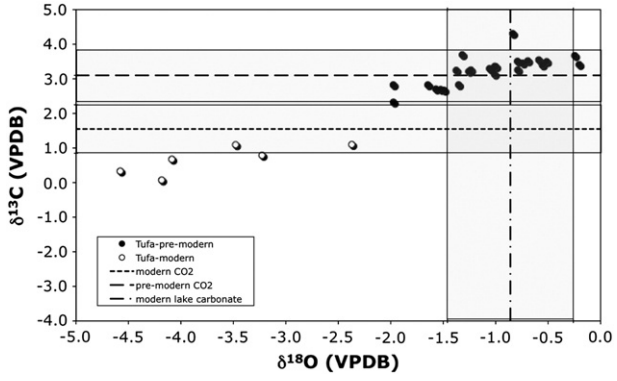

Fig. 5. The $\delta^{13}C$ (PDB) and $\delta^{18}O$ (PDB) values of lake tufa from Cari-Laufquén. The $\delta^{13}C$ values are compared to calculated values of carbonate at 20±5°C using the carbonate–CO_2 fractionation factors from Romanek et al. (1992), for modern (horizontal fine dash) and pre-modern (horizontal coarse dash) CO_2. The $\delta^{18}O$ values are compared to calculated values of carbonate (vertical dash-dot) at 20±5°C formed in the presence of modern lake water, using the carbonate–H_2O fractionation factor from Kim and O'Neil (1997).

Unit A

Unit A (<6 m thick) is quite varied lithologically. The base exposed at CL-17 (Fig. 6) consists of massive, pale-brown silt and fine sand. The middle of Unit A exposed in three sections (Fig. 6: CL-17, -18, -22) is composed of variably cemented sand and gravel. The great variety of sedimentary structures found in the sands include planar bedding, wave-rippled cross-beds, oscillatory ripples, and pinch-and-swell structures. Sand beds in CL-17 (Fig. 6; 1.6 to 3.4 m) commonly display soft sediment deformation features, including ball-and-pillow structures. Ostracodes are locally common. Ostracod assemblages from the area have been described previously by Whatley and Cusminsky (1999), and were not reanalyzed here. The gravels of middle Unit A (Fig. 7: CL-18, -22) are sub to well-rounded, <5 cm thick, and fine to thick bedded. The matrix tends to be coarse sand. A few are flat-pebble shingle gravels. Induration is variable, with cementation by both carbonates and Fe-oxides.

The upper part of Unit A consists of pale brown, laminated silt with local sandy, calcareous partings often containing ostracodes. The top of Unit A is truncated in sections CL-18 and 20 by the basal gravels of Unit B.

Three radiocarbon dates, two from ostracodes (Table 1 and Fig. 6: CL-17d, -18b) and one from a reworked chip of carbonate (CL-18k), all fall >36,000 ^{14}C yr BP. Dates from reworked pieces of tufa found in gravels of the lowway and highway shorelines (Fig. 2 and Table 1: CL-29) yield similarly old ages. As discussed in the Lake History section, we interpret such old ages on carbonate with caution, and as probably infinite in age. As such we do not know if Unit A correlates with the gravels of the low and highway shorelines.

Unit B

The deep-water portion of Unit B, well exposed at CL-17 (Fig. 6), consists of pale brown, laminated silt continuous with the siltstone of Unit A below, but it is less sandy and contains no ostracodes. In other sections (Fig. 6: CL-18, -20) at least 6 m higher in elevation, the base of Unit B is marked by a thin (<20 cm) but conspicuous, sub-rounded gravel and flaser-bedded sand. Sediments quickly fine upwards into massive silt and minor sand, which composes the rest of Unit B in the higher elevation sections CL-18, -20, and 22. The top of Unit B is truncated in section CL-22 by the basal gravel of Unit C.

Four radiocarbon dates (Table 1 and Fig. 6: CL-17e, -20a, -22b, c) from ostracodes and calcareous sand and silt partings date the base (~29 ka) to middle (25.7 ka) of Unit B. The upper meter of silt remains undated.

Unit C

Unit C is the highest elevation lacustrine deposit exposed along the Rio Maquinchao. It is marked by a very thin gravel lens cemented by large tufa heads found in situ at CL-22. This is capped by a 40-cm-thick layer of broken tufa florettes, followed by a 0.5-m-thick gravel layer containing reworked tufa fragments. Massive tufa heads cement the top of the gravel. At CL-23, Unit C consists of calcareous, cross-bedded sand capped by much younger alluvial silt (Unit D?). Along the Rio Maquinchao, Unit C ranges in age from 22.2 ka at the base to 19.7 ka at the top (Fig. 6).

The prominent tufa heads of Unit C occur at about the same elevation at several other locations (Fig. 2 and Table 1: CL-5, 7–10) in the basin. The elevation of the main concentration of in situ tufa heads is the same everywhere at 822–824 m (+36 to +38 m acl). However, there is a scatter of fresh, unreworked tufa fragments in surface float up to 831 m (+45 m acl), just 10 m below the very prominent lowway–highway shoreline complex. These tufa heads range in age

https://doi.org/10.1016/j.yqres.2011.07.002 Published online by Cambridge University Press

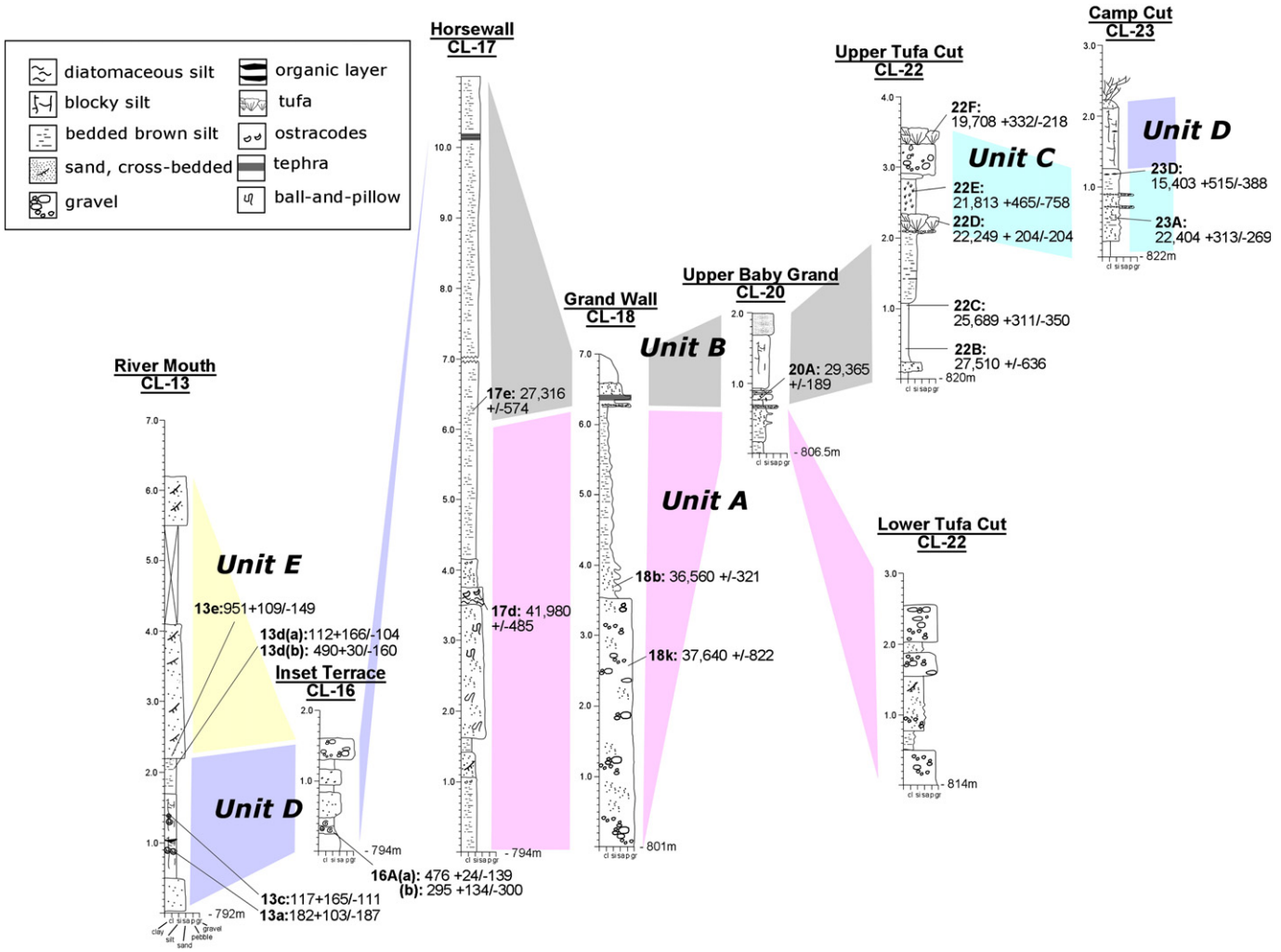

Fig. 6. Main study sections exposed along the Rio Maquinchao (see Fig. 2 for locations). Dates are in calendar years BP (Table 1). Sections are labeled by sample number and field names, with stratigraphic units (A–E) correlated. Base elevation of section and grain size (clay, silt, sand, pebble, gravel) are shown at the bottom of each section.

from 19.1 to 20.7 ka, largely overlapping with the tufa dates from Unit C at the Rio Maquinchao, within the typical error on the dates of ±300 years.

Unit D

Unit D is confined to low elevations along the lowermost reaches of the Rio Maquinchao as an alluvial terrace fill. It can be as much as 4 m thick and consists of pale-green, uncemented, massive to laminated silt and dark gray sand. Organic-rich layers consisting of plant debris are common in the silt. Gravel and sand-filled channels cap Unit D in section CL-13 (Fig. 6). Shells of Lymnaeids, Planorbids, and Succineids are also common in the silt. Dates from the shells range from 117 to 476 cal yr BP (Table 1).

Unit E

Unit E represents the lowest elevation lake deposits (792–798.2 m, or +6 to +12 m acl) exposed along the Rio Maquinchao. Unit E is composed of coarse-grained, bedded sand formed in large-scale (>2 m) back-set beds capped by planar topsets. One shell date obtained from sand at the very base of Unit E came out older at 950 cal yr BP (Table 1 and Fig. 6: CL-13e) than dates from underlying Unit D. We view this shell as reworked; it is a Succineid, a semi-aquatic snail common in Unit D but not known to grow in lakes (Barker, 2001).

Oxygen isotopic composition of waters and carbonate

Springs around and east of Cari-Laufquén, as well as the Rio Maquinchao flowing into the lakes, yield $\delta^{18}O$ (SMOW) and δD (SMOW) values ranging between −13.1 to −10‰ and −97 to −85‰, respectively (Table 3). These waters plot along the global meteoric water line, indicating they are unevaporated (Fig. 7a). Waters from Lago Chico yield higher values, and Lago Grande, the hydrologic terminus of the system, the highest values at +0.5 and −25‰, respectively. The Rio Maquinchao and lake waters plot along a straight line ($r^2 = 0.99$) with a slope of ~5.7, an indication of evaporation (Fig. 7a). $\delta^{18}O$ and δD values of spring and small creek samples decrease westward ($r^2 = 0.82$) over a roughly 150 km distance. All of these springs occur in low mountains hydrographically isolated from the Andes farther to the east (Fig. 7b), and therefore reflect local rain and snowfall, and not runoff from the high Andes.

Historic tufa returned both a broader range and lower $\delta^{18}O$ (PDB) values of −5 to −2‰ than late-glacial tufa from the +38 m shoreline of −2 to −1‰ (Table 3; Fig. 5). At 20±5°C, modern Lago Grande would produce carbonates with $\delta^{18}O$ values (PDB) of −0.9 at equilibrium, slightly higher than the observed values for recent tufas but similar to those from tufa of the ancient (Unit C: +36 to +38 m) lake. Hence, both the modern and ancient lake are and were highly evaporated with respect to inflowing water.

https://doi.org/10.1016/j.yqres.2011.07.002 Published online by Cambridge University Press

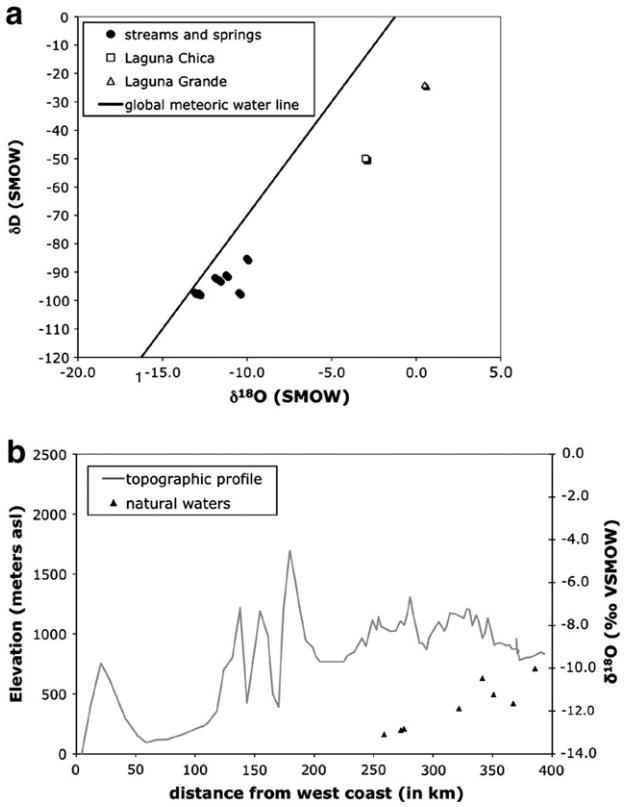

Fig. 7. a) The $\delta^{18}O$ (SMOW) and δD (SMOW) of water in and around Cari-Laufquén, compared to the global meteoric water line, and b) $\delta^{18}O$ (SMOW) values of small springs and creeks around and west of Cari-Laufquén, with a generalized topographic profile for comparison. The sample sites are hydrographically isolated from the Andes, and therefore reflect local rain and snowfall. Elevation profile obtained from traced path along approximately 41°S over SRTM3 DEM (90-m spacing) data.

Discussion

Lake history

In general, we discern at least three periods of lake-level rise, but only the two younger episodes are datable (Fig. 8). The oldest and highest surface paleolake feature is represented by the 847 m (+61 m acl) shoreline. We interpret the >40 ka chips of tufa found in the shoreline gravels as infinite in age, given the well-known propensity for fine-grained carbonate such as tufa to absorb very small (<1%) but measurable amounts of CO_2. We do not know how the +61 m shoreline relates to Unit A exposed at the base of the Rio Maquinchao section. Unit A represents a fining-upward lake transgression from fluvio-deltaic and shoreline sands in the middle, to more profundal

Table 3
Stable isotopic results from Cari-Laufquén and surrounding areas.

Sample #	$\delta^{18}O$ ‰ (VSMOW)	δD ‰ (VSMOW)	Elevation (m asl)	Location/type
Cl-1	0.5	−24	786	Lago Grande, N side
CL-6	−3.0	−50	825	Lago Chica, S side
CL-30	−10.02	−85	833	Rio Maquinchao above Chica
CL-32	−11.65	−93	872	Tap water from Ing. Jacobacci
CL-33	−11.23	−91	904	Large seep
CL-34	−10.47	−97	962	Seep
CL-35	−11.89	−92	1142	Seep
CL-36	−12.84	−98	1027	Small creek
CL-37	−12.90	−97	1070	Seep
CL-38	−13.10	−97	942	Seep

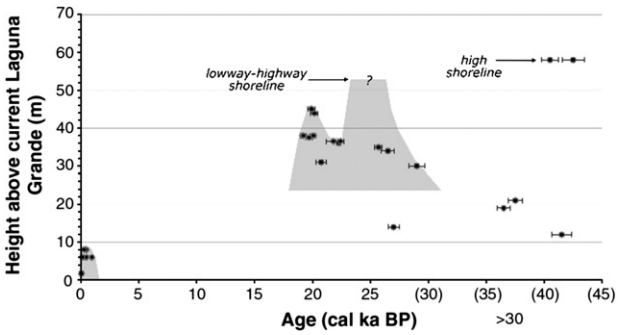

Fig. 8. Summary of Cari-Laufquén lake-level history. The dates in parenthesis are plotted as finite ages but are regarded as minima. Points indicate ages (in cal yr BP; see Table 1) and height above current level of Laguna Grande (786 m asl in 2007).

siltstone above. Unit A returned ages >36.5 ka, which again we view as probable infinite ages.

Unit B marks a second major lake transgression (Fig. 8) that reached at least to 831 m (+45 m acl) and perhaps to the lowway–highway shoreline complex at 841 (+55 m acl). At the lowest section (Fig. 6; CL-17) the deep-water laminated silt of Unit A grades uninterrupted into the same lithology in Unit B, suggesting continuous deepwater deposition at this site from >40 ka up through Unit B starting at around 27 ka. This continuous deepwater environment could explain the lack of gravel marker bed seen at CL-17 in the Unit A–B contact (Fig. 6). At higher elevations (Fig. 6, CL-18 and higher), the basal gravel of Unit B marks a clear transgression past this elevation at about 807 m (+21 m acl) starting 27–29 ka. In CL-22 (0.3 to 2.1 m), laminated siltstone was deposited above the gravel, probably representing the deepest phase in this lake cycle. The siltstone sits at 821–822 (+35–36 m acl), and since it was deposited offshore, the lake must have been deeper than this. It is conceivable that this deep lake phase produced the lowway–highway shoreline complex at 839 m (+53 m acl) but this must be tested by direct dating of the shoreline by optically stimulated luminescence (OSL) or some other means. Material suitable for radiocarbon has not been found associated with the lowway–highway shoreline complex. At present, the age of this deep phase of the lake can be constrained between 26.5 ka near the base of the siltstone in CL-22 (Fig. 6), and 22.3–22.4 ka, the age of the base of Unit C at CL-22/-23.

The Unit B–C contact is exposed only at CL-22 (Fig. 6, at +2.1 m in the section, or 844 m) where very thin basal gravel marks the base of Unit C. The top of this gravel is cemented by large tufa heads, dated at 22,250 cal yr BP (CL-22d). This denotes a regression of the lake so that only shallow water covered the site. Another gravel/tufa couplet caps the measured CL-22 section, perhaps denoting a minor lake oscillation about the 823 m (+37 m acl) elevation. Unit C spans 22.3 to 19.7 ka at this location. At other locations tufa from about this elevation dates to as young as 19,200 cal yr BP (CL-07). At nearby CL-23, a radiocarbon date on lacustrine bulk calcareous sand came back as 22,400 cal yr BP (CL-23a). The overlying date of 15,400 cal yr BP (CL-23d) in that section is from post-depositional diagenetic calcite, and therefore a minimum age for Unit C at that location. Assuming that the tufa and gravel formed in waters no more than a few meters deep, we take this combined evidence to mean that the lake regressed to about 825 m by 22.3–22.4 ka, oscillated around this level until 19.1 ka, then regressed thereafter, as evidenced by the total lack of lacustrine sediment capping the highest tufa in CL-22.

There is a hiatus in lacustrine deposition of almost 18 ka before Unit D was laid down and Unit E was deposited within the last 500 years. There is no evidence that deep lakes developed during this long hiatus such as those present >19 ka. However, the very shallow record is not well exposed, and it is possible, even likely, that our

https://doi.org/10.1016/j.yqres.2011.07.002 Published online by Cambridge University Press

characterization there is incomplete. We suspect, based on the oxygen isotopic evidence, that the lake may have dried or nearly dried sometime after 18 ka, before its transgression during Unit E time. $\delta^{18}O$ (VPDB) values of tufa carbonate from the +36–38 m shoreline (~19 ka) is higher than values from near-modern tufa just above the much shallower modern lake (Fig. 5). This pattern could be explained by a drying or near-drying of the post-18 ka lake, followed by refilling of the lake during Unit E time or some other unidentified post-18 ka lake transgression.

Unit D is exposed in terrace fill all along the lowermost Rio Maquinchao, and this combined with the presence of interbedded sand and gravel, semi-aquatic (Succineids) and pond (Planorbids) snails, and carbonized vegetation indicates Unit D is alluvial. The exposed portions all date to the last 500 years.

Unit E is well exposed at CL-13 (Fig. 6), and is clearly a beach ridge complex with beach barrier top set and back set beds (Fig. 4b) developed on top of Unit D. The lake reached about 798 m (+12 m acl). This lake oscillation started and ended within the last few hundred years. The uncertainties in ^{14}C calibration for the last 400 years do not allow a more precise analysis of lake history timing.

A post-bomb date on tufa (CL-02) within 1.7 m of the 2007 lake shows that lake level has dropped a few meters to its present level over the last few decades. This is consistent with the oxygen isotope evidence from these young tufas that show lower values (Fig. 5) than that predicted to form from the modern lake. This relationship could be explained by gradual lake drop due to evaporation over the past several decades.

Regional significance

The Laguna Cari-Laufquén record is the first detailed shoreline study in southern South America that extends well beyond the Holocene. The only other detailed shoreline study in the region from Lago Cardiel (52°S) focused on the Holocene (Stine and Stine, 1990). This lake fluctuated significantly in size during the Holocene, but the higher, pre-Holocene shorelines remain undated.

As with our Cari-Laufquén record, most records across southern South America and the nearby Pacific point to colder and in many cases wetter conditions during the LGM (Fig. 9) (e.g., Denton et al., 1999; Moreno et al., 1999; Kaplan et al., 2004; Schaefer et al., 2006). Pacific sea-surface temperatures at the latitude of Cari-Laufquén are coldest in the LGM, and warm abruptly at 19 ka, coincident with major lake-level fall from 38.5 m (Lamy et al., 2007; Fig. 9). Glaciers in the Chilean Lake District (41°S, Fig. 1) studied by Denton et al. (1999) show a maximum extent at the same time as the LGM-age highstand at Cari-Laufquén. Pollen records from the same area are interpreted to show much moister conditions for the period roughly 23 to 16 ka (Moreno et al., 1999). In southern Patagonia (45°S) Markgraf et al. (2007) documented a range of evidence from a sediment core at Lago Pollux (Fig. 1), a glacially fed closed-basin lake in southern Chile. They identified moist conditions at Lago Pollux just before 18 ka, and drier conditions 18 to 14 ka. Core and seismic evidence (Markgraf, 1993; Gilli et al., 2005) from Lago Cardiel agrees with shoreline evidence (Stine and Stine, 1990) for significant Holocene-age changes in lake depth, but the core does not extend beyond ~12 ka. South of Lago Cardiel, Laguna Potrok Aike apparently deepened during the LGM (Gilli et al., 2005; Haberzettl et al., 2007; Anselmetti et al., 2008), but the age of the shorelines around the lake remain unclear.

The same authors offer a range of explanations for extended glaciers and expanded lakes during the LGM across the region. Glacial modeling reproduces the LGM ice extent with both temperature depression and precipitation increases, but shows a stronger sensitivity to temperature (e.g., Hulton et al., 2002). The majority of non-glacial records are interpreted to reflect cooler temperatures *and* increased moisture as a cause of expansion and freshening of lakes in the LGM. As an example, Moreno et al. (1999) invoke both a 6–7°C drop in temperature and a doubling of rainfall to induce significant treeline depression and the expansion of *Nothofagus dombeyi* parkland in the Chilean Lake District. Nearly all recent papers invoke an equatorward shift of the Antarctic circumpolar current during the LGM, and corresponding northward shift of the westerlies, as the cause of greater effective moisture (e.g., Hulton et al., 2002; Wainer et al., 2005; Markgraf et al., 2007). In support of this, Markgraf et al. (2007) cite the evidence for dry conditions between 14 and 11 ka in southernmost Patagonia at Lago Pollux and Lago Cardiel (Fig. 1). Markgraf et al. (2007) explains this as a shift in the position of the westerly storm tracks so far north that southernmost Patagonia (>45°S) actually dried in the LGM. However, since lake levels and lake conditions during the LGM remain undocumented at both Pollux and Cardiel, one of the strongest arguments in favor on the shifting westerlies hypothesis remains equivocal.

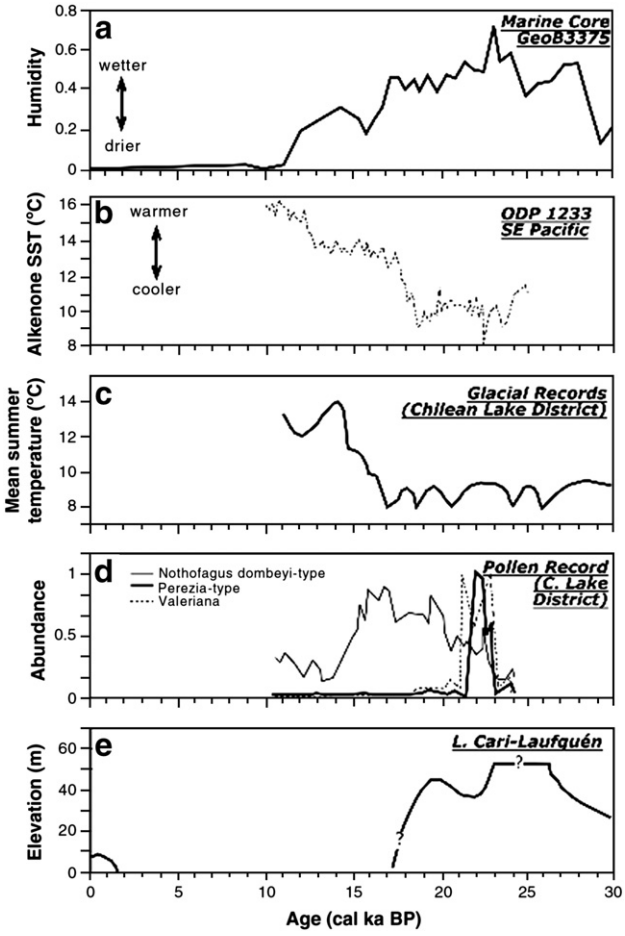

Fig. 9. Comparison of Laguna Cari-Laufquén lake history to other regional records (see Fig. 1 for locations). a) The north Chilean humidity index obtained from grain-size analyses in marine core GeoB3375 (27°28′S, 71°15′W) after Stuut and Lamy (2004); b) Alkenone SST record from marine core 1233 (41°00′S, 74°27′W) after Lamy et al. (2007); c) Chilean Lake District (40°30′–42°25′S; 72°25′–73°45′ W) paleotemperature record from Denton et al. (1999) glacial study; d) Schematic Chilean Lake District selected pollen record after Moreno et al. (1999) core PM13. Abundance for each pollen type is shown relative to maximum and minimum amounts found in the core; and e) Cari-Laufquén lake level changes relative to modern Laguna Grande (786 m asl in 2007).

A challenge to the hypothesis that the position and strength of the westerlies controls all mid-latitude rainfall comes from Garreaud (2007). This study examined monthly and yearly rainfall anomalies in relation to zonal wind in the lower troposphere (850 hPa) and upper troposphere (300 hPa). They found that rainfall and westerly winds are highly correlated on the windward (western) side of the Andes, but anti-phased on the Patagonian or eastern side. In short, the stronger the westerly winds, the stronger the rainshadow effect by

https://doi.org/10.1016/j.yqres.2011.07.002 Published online by Cambridge University Press

the Andes, the lower the rainfall in Patagonia. This anti-phasing is confirmed by the rather meager climate records in Patagonia (e.g., Moy et al., 2009), which show that Patagonian rainfall derives mainly from the Atlantic, not Pacific, and is suppressed by strong westerly winds (Mayr et al., 2007). The influence of Atlantic moisture at the latitude of Cari-Laufquén is clearly visible in the gradual decrease in $\delta^{18}O$ values of meteoric water from east to west toward the Andes (Fig. 7b). Were the Pacific Ocean the source of moisture in the area, then $\delta^{18}O$ values would follow the opposite pattern and decrease eastward, away from the source. The anti-phasing of modern rainfall makes the correlation between apparent wet and dry phases west and east of the Andes all the more puzzling, as already pointed out by Moy et al. (2009) for the Little Ice Age and Medieval Warm Phase. Our observations extend the puzzle to the last glacial maximum.

One possible explanation of the correlation of records west and east of the Andes is that the expansion of Cari-Laufquén and other lakes is driven mainly by temperature decrease and not rainfall increase. The relative contribution of rainfall and temperature changes that lake area change awaits hydrologic modeling, which will be the focus of follow-up papers.

Modeling simulations (PMIP2) by Rojas et al. (2009) show no significant latitudinal shift in the jet stream position during the LGM, but they do show increased storm activity (a higher density of embedded cyclones) in winter mid-latitudes (25° to 45°S), as well as decreased westerly wind strength during the LGM. Both these features of the simulations might explain the observed lake expansion at Cari-Laufquén, since they would enhance rainfall from the Atlantic in Patagonia. At the same time increased storm densities could account for wetter conditions on the Pacific side of the Andes, even though the westerly wind-strength was diminished. A robust test of this explanation awaits documentation of more records at these latitudes east of the Andes, which at present are very limited, and especially along the Atlantic Coast

It is possible that the most recent lake oscillation seen at Cari-Laufquén corresponds to the Little Ice Age during the 17th century, when others have also suggested a period of wetter conditions in this area (Moy et al., 2008). However, uncertainties in the ^{14}C calibration for the last 400 years preclude making a definite link between Cari-Laufquén's most recent expansion and external causes.

Moving equatorward into the easterly-dominated latitudes, the chronology of lakes in the subtropics of South America is fundamentally different from that at Cari-Laufquén and other Patagonian lakes. In this region, the largest lake expansions occur in the late glacial (17–10 ka) rather than during the LGM (Grosjean, 1994; Mourguiart et al., 1997; Seltzer, et al., 2002; Jennerjahn et al., 2004; Placzek et al., 2006; Weng et al., 2006). Rainfall in the subtropics appears to be controlled by North Atlantic temperatures and ice releases (Heinrich events) perhaps amplified by ENSO variation (Placzek et al., 2006; Blard et al., 2009). For example, from the high Andes of Bolivia, Placzek et al. (2006) show that megalakes (>55 km^2) were most expansive (up to 5× modern in area) in the late glacial and smaller (2× modern) during the LGM. Modeling suggests that these expansions may be related to North Atlantic cooling, in this case during Heinrich 1 and the Younger Dryas periods (Grosjean, 1994; Chiang et al., 2003; Blard et al., 2009). Evidence from paleowetlands in the Atacama Desert of northwest Chile also show these double deglacial wet periods, and no LGM-age wet event (Quade et al., 2008). This is in strong contrast to the LGM-age highstand at Cari-Laufquén, and it suggests fundamentally different response of climate between low and high latitudes.

Globally, the lake-level chronology for Cari-Laufquén follows the pattern of substantial expansion displayed by most high to mid-latitude (>35°N) lakes during the LGM. Prime examples of this from well-dated shoreline sequences include Lakes Bonneville and Lahontan in western North America (Eardley et al., 1957; Broecker and Kaufman, 1965; Benson et al., 1990; Oviatt et al., 1992; Godsey et al., 2005; Adams, 2010), Lake Konya in Turkey (Roberts, 1983; Fontugne et al., 1999), and Lake Lisan in Israel (Kaufman et al., 1992; Bartov et al., 2002; Torfstein et al., 2008). Although there is greater variability in the timing of the North American and Lake Lisan records, where in many cases the highstand occurred during the late glacial, all of these records experienced large lake expansions during the LGM. Modeling conducted on most of these systems (Benson et al., 1990; Bartov et al., 2002; Jones et al., 2007) points to lower temperatures combining with higher rainfall to produce larger lakes. As with South America, the emphasis has been on equatorward shift of the westerlies as the cause for lake expansion (Antevs, 1948; Benson and Thompson, 1987; Hostetler and Benson, 1990; Oviatt, 1997). We would suggest that temperature depression combined with intensification of the rainfall—rather than a poleward shift—in the westerlies belt could equally account for this hemispheric symmetry of lake-level records during the LGM (Quade and Broecker, 2009). As in South America, well-dated shoreline records obtained from very high latitudes should help in distinguishing these explanations.

Supplementary materials related to this article can be found online at doi:10.1016/j.yqres.2011.07.002

Acknowledgments

We thank David Dettman for help in the laboratory, and Julie Cole and Julio Betancourt for feedback on this manuscript. This work was supported by the COMER Science and Education Foundation.

References

Adams, K.D., 2010. Lake levels and sedimentary environments during deposition of the Trego Hot Springs and Wono tephras in the Lake Lahontan basin, Nevada, USA. Quaternary Research 73, 119–129.
Anselmetti, F., Ariztegui, D., De Batist, M., Gebhardts, A., Haberzettl, T., Niessen, F., Ohlendorf, C., Zolitschka, B., 2008. Environmental history of southern Patagonia unraveled by the seismic stratigraphy of Laguna Potrok Aike. Sedimentology 1–20.
Antevs, E., 1948. The Great Basin, with emphasis on glacial and post-glacial times—climate changes and pre-white man. Bulletin of the University of Utah Biological Services 38, 168–191.
Barker, G., 2001. The biology of terrestrial molluscs. In: Barker, G.M. (Ed.), Gastropods on Land: Phylogeny, Diversity and Adaptive Morphology. CABI Publishing, Oxon, UK, pp. 139–142.
Bartov, Y., Stein, M., Enzel, Y., Agnon, A., Reches, Z., 2002. Lake levels and sequence stratigraphy of Lake Lisan, the Late Pleistocene precursor of the Dead Sea. Quaternary Research 57, 9–21.
Benson, L., Currey, D., Dorn, R., Lajoie, K., Oviatt, C., Rombinson, S., Smith, G., Stine, S., 1990. Chronology of expansion and contraction of four Great Basin lake Systems during the past 35,000 years. Palaeogeography, Palaeoclimatology, Palaeoecology 78, 241–286.
Benson, L., Thompson, R., 1987. Lake-level variation in the Lahontan Basin for the past 50,000 years. Quaternary Research 28, 69–85.
Blard, P., Lavé, J., Farley, K., Fornari, M., Jiménez, N., Ramierz, V., 2009. Late local glacial maximum in the Central Altiplano triggered by cold and locally-wet conditions during the palaeolake Tauca episode (17–15 ka, Heinrich 1). Quaternary Science Reviews 28, 3414–3427.
Broecker, W., Kaufman, A., 1965. Radiocarbon chronology of Lake Lahontan and Lake Bonneville II. Geological Society of America Bulletin 76, 537–566.
Cheng, H., Edwards, L., Hoff, J., Gallup, C., Richards, D., Asmerom, Y., 2000. The half-life of uranium-234 and thorium-230. Chemical Geology 169, 17–33.
Cheng, H., Edwards, R.L., Shen, C.C., Woodhead, J., Hellstrom, J., Wang, Y.J., Kong, X.G., Wang, X.F., 2008. A new generation of Th-230 dating techniques: tests of precision and accuracy. Geochimica et Cosmochimica Acta 72, A157-A157.
Cheng, H., Fleitmann, D., Edwards, R.L., Wang, X.F., Cruz, F.W., Auler, A.S., Mangini, A., Wang, Y.J., Kong, X.G., Burns, S.J., Matter, A., 2009. Timing and structure of the 8.2 ky event inferred from $\delta^{18}O$ records of stalagmites from China, Oman and Brazil. Geology 37, 1007–1010.
Chiang, J., Biasutti, M., Battisti, D., 2003. Sensitivity of the Atlantic Intertropical Convergence Zone to Last Glacial Maximum boundary conditions. Paleoceanography 18, 1094–1111.
Denton, G., Lowell, T., Moreno, P., Andersen, B., Schluchter, C., 1999. Interhemispheric linkage of paleoclimate during the last glaciation. Geografiska Annaler Series A 81A, 167–229.
Eardley, A., Gvosdetsky, V., Marsell, R., 1957. Hydrology of Lake Bonneville and sediments and soils of its basin. Geological Society of America Bulletin 68, 1141–1201.
Edwards, R.L., Chen, J.H., Wasserburg, G.J., 1987. ^{238}U, ^{234}U, ^{230}Th, ^{232}Th systematics and the precise measurement of time over the past 500,000 years. Earth and Planetary Science Letters 81, 175–192.

Fontugne, M., Kuzucuoglu, M., Karabiyikoglu, C., Hatte, C., Pastre, J., 1999. From pleniglacial to Holocene: a ^{14}C chronostratigraphy of environmental changes in the Konya Plain, Turkey. Quaternary Science Reviews 18, 573–591.
Galloway, R.M., Markgraf, V., Bradbury, J.P., 1988. Dating of shorelines of lakes in Patagonia, Argentina. Journal of South American Earth Science 1, 195–198.
Garreaud, R., 2007. Precipitation and circulation covariability in the extratropics. Notes and Correspondence 20, 4789–4797.
Gilli, A., Anselmetti, F., Ariztegui, D., Beres, M., McKenzi, J., Markgraf, V., 2005. Seismic stratigraphy, buried beach ridges and contourite drifts: the Late Quaternary history of the closed Lago Cardiel basin, Argentina (49°S). Sedimentology 52, 1–23.
Godsey, H., Currey, D., Chan, M., 2005. New evidence for an extended occupation of the Provo shoreline and implications for regional climate change, Pleistocene Lake Bonneville, Utah, USA. Quaternary Research 63, 212–223.
Graham, S., Famiglietti, J., Maidment, D., 1999. Five-minute, 1/2°, and 1° data sets of continental watersheds and river networks for use in regional and global hydrologic and climate system modeling studies. Water Resources Research 35, 583–587.
Grosjean, M., 1994. Paleohydrology of Laguna Lejía (north Chilean Altiplano) and climatic implications for late-glacial times. Palaeogeography, Palaeoclimatology, Palaeoecology 109, 89–100.
Haberzettl, T., Corbella, H., Michael, F., Janssen, S., Lucke, A., Mayr, C., Ohlendorf, C., Schabitz, F., Schleser, G., Wille, M., Wulf, S., Zolitschka, B., 2007. Late glacial and Holocene wet–dry cycles in southern Patagonia: chronology, sedimentology and geochemistry of lacustrine record from Laguna Potrok Aike, Argentina. The Holocene 17, 297–310.
Held, I., Soden, B., 2006. Robust responses of the hydrological cycle to global warming. Journal of Climate 19, 5686–5699.
Hostetler, S., Benson, L., 1990. Paleoclimatic implications of the high stand of Lake Lahontan derived from models of evaporation and lake level. Climate Dynamics 4, 207–217.
Hulton, N., Purves, R., McCulloch, R., Sugden, D., Bentley, M., 2002. The Last Glacial Maixmum and deglaciation in southern South America. Quaternary Science Reviews 21, 233–241.
Jennerjahn, T., Ittekkot, V., Arz, H., Behling, H., Patzold, J., Wefer, G., 2004. Asynchronous terrestrial and marine signals of climate change during Heinrich events. Science 306, 2236–2239.
Jones, M., Roberts, C., Leng, M., 2007. Quantifying climatic change through the last glacial–interglacial transition based on lake isotope palaeohydrology from central Turkey. Quaternary Research 67, 463–473.
Kaplan, M., Ackert Jr., R., Singer, B., Douglass, D., Kurz, M., 2004. Cosmogenic nuclide chronology of millennial-scale glacial advances during isotope stage 2 in Patagonia. Geological Society of America Bulletin 116, 308–321.
Kaufman, A., Yechieli, Y., Gardosh, M., 1992. Re-evaluation of the lake-sediment chronology in the Dead Sea basin, Israel, based on new 230Th/U dates. Quaternary Research 38, 292–304.
Kim, S.-T., O'Neil, J.R., 1997. Equilibrium and non-equilibrium oxygen isotope effects in synthetic carbonates. Geochimica et Cosmochimica Acta 61, 3461–3475.
Lamy, F., Kaiser, J., Arz, H., Hebbeln, D., Ninnemann, U., Timm, O., Timmermann, A., Toggweiler, J., 2007. Modulation of the bipolar seesaw in the Southeast Pacific during Termination 1. Earth and Planetary Science Letters 259, 400–413.
Lowell, T., Heusser, C., Andersen, B., Moreno, P., Hauser, A., Heusser, L., Schluchter, C., Marchant, D., Denton, G., 1995. Interhemispheric correlation of late Pleistocene glacial events. Science 269, 141–149.
Markgraf, V., 1993. Paleoenvironments and paleoclimates in Tierra del Fuego and southernmost Patagonia, South America. Palaeogeography, Palaeoclimatology, Palaeoecology 102, 53–68.
Markgraf, V., 1998. Past climates of South America. Climates of the Southern Continents: Present, Past and Fugure. John Wiley and Sons Ltd., pp. 249–264.
Markgraf, V., Whitlock, C., Haberle, S., 2007. Vegetation and fire history during the last 18,000 cal yr B.P. in Southern Patagonia: Mallin Pollux, Coyhaique, Province Aisen. Palaeogeography, Palaeoclimatology, Palaeoecology 254, 492–507.
Mayr, C., Wille, M., Haberzettl, T., Fey, M., Janssen, S., Lücke, A., Ohlendorf, C., Oliva, G., Schäbitz, F., Schleser, G.H., Zolitschka, B., 2007. Holocene variability of the Southern Hemisphere westerlies in Argentinian Patagonia (52°S). Quaternary Science Reviews 26, 579–584.
Mercer, J., 1984. Climate processes and climate sensitivity in simultaneous climatic change in both hemispheres and similar bipolar inter-glacial warming: evidence and implications. American Geophysical Union, Geophysical Monograph 29, 20–313.
Miller, A., 1976. The climate of Chile in climates of Central and South America. World Survey of Climatology 113–130.
Moreno, P., Lowell, T., Jacobson, G., Denton, G., 1999. Abrupt vegetation and climate changes during the last glacial maximum and last termination in the Chilean Lake District: a case study from Canal de la Puntilla (41°S). Geografiska Annaler Series A 81A, 285–312.
Morrison, R., 1978. Quaternary soil stratigraphy—concepts, methods, problems. In: Mahaney, W.C. (Ed.), Quaternary Soils: Norwich, Geoabstracts, pp. 77–108.
Morrison, R.B., 1991. Quaternary stratigraphic, hydrologic, and climatic history of the Great Basin, with emphasis on Lakes Lahontan, Bonneville, and Tecopa. In: Morisson, R.B. (Ed.), Quaternary Nonglacial Geology; Conterminous U.S.: Geological Society of America. The Geology of North America, Boulder, Colorado, pp. 283–320.
Mourguiart, P., Argollo, J., Correge, T., Martin, L., Montenegro, M., Sifeddine, A., Wirrmann, D., 1997. Changements limnologiques et climatologiques dans le basin du lac Titicaca (Bolivie) depuis 30 000 ans. Earth and Planetary Sciences 325, 139–146.
Moy, M., Dunbar, B., Moreno, I., Francois, P., Villa-Martínez, R., Mucciarone, M., Guilderson, P., Garreaud, D., 2008. Isotopic evidence for hydrologic change related to the westerlies in SW Patagonia, Chile, during the last millennium. Quaternary Science Reviews 27, 1335–1349.
Moy, M., Moreno, P.I., Dunbar, B., Kaplan, M.R., Francois, P., Villalba, R., Hazerbertl, T., 2009. Climate change in southern America during the last two millennia. Past Climate Variability in South America and Surrounding Regions. : In: Vimeaux, et al. (Ed.), Developments in Paleoenvironmental Research, 14. Springer, pp. 353–393.
Oviatt, C., 1997. Lake Bonneville fluctuations and global climate change. Geology 25, 155–158.
Oviatt, C., Currey, D., Sack, D., 1992. Radiocarbon chronology of Lake Bonneville, Eastern Great Basin, USA. Palaeogeography, Palaeoclimatology, Palaeoecology 99, 225–241.
Placzek, C., Quade, J., Patchett, P.J., 2006. Geochronology and stratigraphy of late Pleistocene lake cycles on the southern Bolivian Altiplano: implications for causes of tropical climate change. Geological Society of America Bulletin 118, 515–532.
Quade, J., Broecker, W., 2009. Dryland hydrology in a warmer world: lessons from the Last Glacial period. The European Journal Special Topics 176, 21–36.
Quade, J., Rech, J., Betancourt, J., Latorre, C., Rylander, K., Fisher, T., 2008. Paleowetlands and regional climate change in the central Atacama Desert, northern Chile. Quaternary Research 69, 343–360.
Reimer, P., Baillie, L., Bard, E., Bayliss, A., Beck, W., Blackwell, G., Bronk Ramsey, C., Buck, E., Burr, S., Edwards, L., Friedrich, M., Grootes, M., Guilderson, P., Hajdas, I., Heaton, J., Hogg, G., Hughen, A., Kaiser, F., Kromer, B., McCormac, G., Manning, W., Reimer, W., Richards, A., Southon, R., Talamo, S., Turney, M., van der Plicht, J., Weyhenmeyer, E., 2009. IntCal09 and Marine 09 radiocarbon age calibration curves, 0–50,000 years cal BP. Radiocarbon 51, 1111–1150.
Reissig, M., Trochine, C., Queimalinos, C., Balsiero, E., Modenutti, B., 2006. Impact of fish introduction on planktonic food webs in lakes of the Patagonian Plateau. Biological Conservation 132, 437–447.
Roberts, N., 1983. Age, palaeoenvironments, and climatic significance of late Pleistocene Konya lake, Turkey. Quaternary Research 19 (154–171), 352–355.
Rojas, M., Moreno, P., Kageyama, M., Crucifix, M., Hewitt, C., Abe-Ouchi, A., Ohgaito, R., Brady, C., Hope, P., 2009. The Southern Westerlies during the last glacial maximum in PMIP2 simulations. Climate Dynamics 32, 525–548.
Romanek, C.S., Grossman, E.T., Morse, J.W., 1992. Carbon isotopic fractionation in synthetic aragonite and calcite: effects of temperature and precipitation rate. Geochimica et Cosmochimica Acta 419–430.
Schaefer, J., Denton, G., Barrell, D., Ivy-Ochs, S., Kubik, P., Andersen, B., Phillips, F., Lowell, T., Schluchter, C., 2006. Near-synchronous interhemispheric termination of the last glacial maximum in mid-latitudes. Science 312, 1510–1513.
Seltzer, G., Rodbell, D., Baker, P., Fritz, S., Tapia, P., Rowe, H., Dunbar, R., 2002. Early warming of tropical South America at the last glacial–interglacial transition. Science 31, 1685–1686.
Street, F.A., Grove, A.T., 1979. Global maps of lake-level fluctuations since 30,000 yr B.P. Quaternary Research 12, 83–118.
Stine, S., Stine, M., 1990. A record from Lake Cardiel of climate change in southern South America. Nature 345, 705–708.
Stuiver, M., Reimer, R.W., 1993. Extended ^{14}C database and revised CALIB radiocarbon calibration program. Radiocarbon 35, 215–230.
Stuut, J., Lamy, F., 2004. Climate variability at the southern boundaries of the Namib (southwestern Africa) and Atacama (northern Chile) coastal deserts during the last 120,000 yr. Quaternary Research 62, 301–309.
Torfstein, A., Gavrieli, I., Katz, A., Kolodny, Y., Stein, M., 2008. Gypsum as a monitor of the paleo-limnological–hydrological conditions in Lake Lisan and the Dead Sea. Geochimica et Cosmochimica Acta 72, 2491–2509.
Wainer, I., Clauzet, G., Ledru, M., Brady, E., Otto-Bliesner, B., 2005. Last glacial maximum in South America: paleoclimate proxies and model results. Geophysical Research Letters 32, L0872.
Weng, C., Bush, M., Curtis, J., Kolata, A., Dillehay, T., Binford, M., 2006. Deglaciation and Holocene climate change in the western Peruvian Andes. Quaternary Research 66, 87–96.
Whatley, R.C., Cusminsky, G.C., 1999. Lacustrine ostracoda and late Quaternary palaeoenvirnoments from the Lake Cari-Laufquén region, Rio Negro Province, Argentina. Palaeogeography, Palaeolimnology, Palaecology 151, 229–239.